Preparation and Spectral Properties of Oxovanadium(IV), Nickel(II), Copper(II), and Palladium(II) Complexes of Tetraaza[14]annulenes

Kazunori SAKATA,* Mamoru HASHIMOTO, Noriyoshi TAGAMI, and Yukito MURAKAMI*,†

Department of Chemistry, Kyushu Institute of Technology, Tobata-ku, Kitakyushu 804

†*Department of Organic Synthesis, Faculty of Engineering, Kyushu University, Hakozaki, Higashi-ku, Fukuoka 812*

(Received January 7, 1980)

The oxovanadium(IV), nickel(II), copper(II), and palladium(II) complexes of 5,14-dihydrodibenzo[*b,i*]-[1,4,8,11]tetraazacyclotetradecine and 7,8,15,16,17,18-hexahydrodibenzo[*b,j*][1,4,8,11]tetraazacyclotetradecine have been synthesized, and studied by electronic, vibrational, NMR, ESR, and ESCA spectroscopy. The absorption bands appearing in the energy region greater than 16800 cm^{-1} were attributed to $\pi \rightarrow \pi^*$ transitions within a ligand molecule and metal to ligand charge-transfer transitions. The ligand-field bands were not assigned for the present complexes, because all the ligand-field bands were obscured by the $\pi \rightarrow \pi^*$ and charge-transfer bands of high intensity. The metal complexes assume the square-planar configurations since no significant absorption band was detected in the region below 17000 cm^{-1}. A strong band appearing at *ca.* 1620 cm^{-1} was assigned to the C=N stretching mode, and this band was shifted to lower frequency upon metal coordination. A V=O streching band was observed at *ca.* 950 cm^{-1} for the oxovanadium complexes. The oxovanadium, nickel, copper, and palladium complexes showed a single nitrogen 1s peak by ESCA spectroscopy, whereas the metal-free ligand, 5,14-dihydrodibenzo[*b,i*][1,4,8,11]tetraazacyclotetradecine, revealed double nitrogen 1s peaks. ESR spectra were measured in xylene–benzene (2: 1 v/v) as well as in the corresponding ligand matrices at room temperature. Judging from *g* tensors, the copper complexes were confirmed to have D_{2h} coordination symmetry with an unpaired electron in the d_{xy} orbital. On the other hand, vanadium(IV) is in C_{4v} coordination symmetry with an unpaired electron in the $d_{x^2-y^2}$ orbital.

The naturally occurring macrocycles with N_4-donor atoms, porphyrins and corrins, may form metal complexes which involve four conjugated six-membered chelate rings (6^4 type) and three six- and one five-membered chelate rings (6^3-5 type), respectively. However, there are many N_4-macrocycles which can yield metal complexes having other combinations of chelate-ring sizes. The chemistry of metal porphyrins and metal corrins has been widely investigated up to the present time because of their biochemical interest.[1,2]

In the present work, we employed N_4-macrocycles which can form two six- and two five-membered chelate rings of 6-5-6-5 type; a 16 π-macrocyclic ligand, 5,14-dihydrodibenzo[*b,i*][1,4,8,11]tetraazacyclotetradecine (**1**), and a 12 π-macrocycle, 7,8,15,16,17,18-hexahydrodibenzo[*b,j*][1,4,8,11]tetraazacyclotetradecine (**2**). A number of π-electrons placed in the interior molecular skeleton of this type extends from none for the completely saturated system to 16 for complete conjugation.[3] Hiller *et al.*[4] and Green *et al.*[5] reported electronic and vibrational spectra of the nickel(II) and copper(II) of macrocyclic ligands **1** and **2** without assignments of characteristic bands. We characterized the spectral properties of the oxovanadium(IV), nickel(II), copper-(II), and palladium(II) complexes of the present macrocycles by means of electronic, vibrational, ESR, NMR, and ESCA spectroscopy. The characteristic coordination behavior of the present planar ligand has been discussed in reference to the ligand properties of porphyrins.

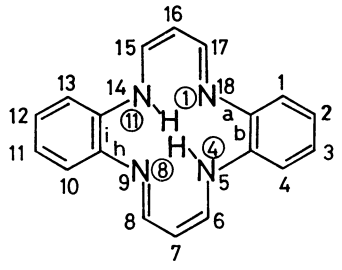

1

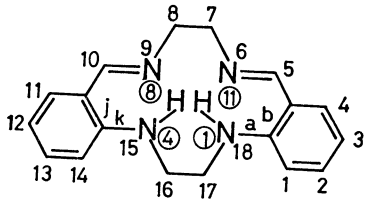

2

Experimental

5,14-Dihydrodibenzo[b,i][*1,4,8,11*]*tetraazacyclotetradecine(1).* Prepared after Hiller *et al.*[4] from 1,2-diaminobenzene (36.5 g) and 2-propynal (18.2 g)[6] in a mixed solvent composed of methanol (90 ml) and *N,N*-dimethylformamide (45 ml). The crystalline solid was washed with methanol (50 ml) and recrystallized from *N,N*-dimethylfomamide as glittering red needles; yield 11.0 g (23%). Found: C, 74.82; H, 5.57; N, 19.55%; M^+, 288.[7] Calcd for $C_{18}H_{16}N_4$: C, 74.98; H, 5.59; N, 19.43%; M, 288.35.

(Dibenzo[b,i][*1, 4, 8, 11*]*tetraazacyclotetradecinato) oxovanadium-(IV).* A mixture of **1** (0.50 g), vanadium (IV) chloride oxide (0.40 g), and *N,N*-dimethylformamide (80 ml) was heated under reflux for 5 h. To the filtrate of the hot mixture was added water (400 ml), and fine brown crystals were recovered; yield 0.47 g (77%). Found: C, 61.69; H, 4.09; N, 15.64%; M^+, 353.[7] Calcd for $C_{18}H_{14}N_4OV$: C, 61.20; H, 3.99; N, 15.86%; M, 353.28.

(Dibenzo[b,i][*1,4,8,11*]*tetraazacyclotetradecinato)nickel(II).* This complex was prepared from **1** (0.25 g) and nickel(II) acetate tetrahydrate (0.30 g) in the presence of sodium acetate trihydrate (0.50 g) and *N,N*-dimethylformamide (23 ml)

after Hiller *et al.*,[4] and recrystallized from *N,N*-dimethylformamide to give glittering violet plates; yield 0.28 g (94%). Found: C, 63.28; H, 4.11; N, 16.21%; M+, 344.[7] Calcd for $C_{18}H_{14}N_4Ni$: C, 62.66; H, 4.09; N, 16.24%; M, 345.05.

(Dibenzo[b,i]*[1,4,8,11]tetraazacyclotetradecinato)copper(II).* This was prepared from **1** (1.00 g) and copper(II) acetate monohydrate (2.25 g) in the presence of sodium acetate trihydrate (1.50 g) and *N,N*-dimethylformamide (100 ml) after Hiller *et al.*,[4] and recrystallized from *N,N*-dimethylformamide to give glittering dark red needles; yield 1.11 g (91%). Found: C, 61.85; H, 4.15; N, 15.98%; M+, 349.[7] Calcd for $C_{18}H_{14}N_4Cu$; C, 61.79; H, 4.03; N, 16.01%; M, 349.88.

(Dibenzo[b,i]*[1,4,8,11]tetraazacyclotetradecinato)palladium (II).* A mixture of **1** (0.50 g), palladium(II) chloride (0.40 g), and *N,N*-dimethylformamide (25 ml) was heated under reflux for 2 h. The hot mixture was filtered, and water (500 ml) was added to the filtrate. The precipitates were separated and washed with water (100 ml) and methanol (10 ml) to give pale brown needles; yield 0.24 g (35%). Found: C, 55.47; H, 3.91; N, 13.26%; M+, 392.[7] Calcd for $C_{18}H_{14}N_4Pd$; C, 55.05; H, 3.59; N, 14.27%; M, 392.74.

7,8,15,16,17,18-Hexahydrodibenzo[b,j]*[1,4,8,11]tetraazacyclotetradecine (2).* 1,2-Ethanediamine (1.2 ml) dissolved in methanol (100 ml) was added in 1.5 h to a mixture of zinc(II) acetate dihydrate (3.07 g), 2,2′-(ethylenediimino)dibenzaldehyde[8] (2.68 g), and methanol (300 ml) under reflux with stirring. The reaction mixture was refluxed for another 2 h with stirring. After the mixture was cooled down with ice–water, the precipitated crystalline solid was recrystallized from chloroform as colorless needles; yield 1.77 g (61%), mp 279—282 °C (dec). Found: C, 74.24; H, 6.90; N, 19.08%; M+, 292.[7] Calcd for $C_{18}H_{20}N_4$: C, 73.94; H, 6.89; N, 19.16%; M, 292.39.

(7,8,16,17-Tetrahydrodibenzo[b,j] [*1,4,8,11]tetraazacyclotetradecinato)oxovanadium(IV).* 1,2-Ethanediamine (1.07 ml) dissolved in methanol (50 ml) was added in 1 h to a mixture of vanadium (IV) chloride oxide (1.70 g), sodium acetate trihydrate (2.10 g), 2,2′-(ethylenediimino)dibenzaldehyde (1.07 g), and methanol (250 ml) under reflux with stirring. The reaction mixture was refluxed for another 1 h with stirring. After the solvent was evaporated off *in vacuo*, the residue was extracted with chloroform (300 ml), concentrated to *ca.* 10 ml *in vacuo*, and brown needles were obtained upon addition of methanol (35 ml); yield 0.08 g (6%). Found: C, 60.08; H, 5.09; N, 15.50%; M+, 357.[7] Calcd for $C_{18}H_{18}N_4OV$: C, 60.51; H, 5.08; N, 15.68%; M, 357.31.

(7,8,16,17-Tetrahydrodibenzo[b,j] [*1,4,8,11]tetraazacyclotetradecinato)nickel(II).* This was prepared from nickel(II) acetate tetrahydrate (2.49 g), 2,2′-(ethylenediimino) dibenzaldehyde (2.68 g), 1,2-ethanediamine (1.3 ml), and methanol (110 ml) after Green *et al.*,[5] and recrystallized from benzene–petroleum ether (3 : 1 v/v) as glittering dark brown needles; yield 2.38 g (68%). Found: C, 62.42; H, 5.05; N, 15.85%; M+, 348.[7] Calcd for $C_{18}H_{18}N_4Ni$: C, 61.93; H, 5.20; N, 16.05%; M, 349.08.

(7,8,16,17-Tetrahydrodibenzo [b,j][*1,4,8,11]tetraazacyclotetradecinato)copper(II).* This was prepared from copper(II) acetate monohydrate (1.00 g), 2,2′-(ethylenediimino)-dibenzaldehyde (1.34 g), 1,2-ethanediamine (0.67 ml), and methanol (40 ml) after Green *et al.*,[5] and recrystallized from benzene–petroleum ether (3 : 1 v/v) to give glittering dark brown plates; yield 0.75 g (42%). Found: C, 60.89; H, 5.09; N, 15.60%; M+, 353.[7] Calcd for $C_{18}H_{18}N_4Cu$: C, 61.09; H, 5.13; N, 15.83%; M, 353.91.

(7,8,16,17-Tetrahydrodibenzo[b,j][*1,4,8,11]tetraazacyclotetradecinato)palladium(II).* 1,2-Ethanediamine (0.33 ml) dissolved in methanol (10 ml) and sodium hydroxide (0.16 g in 0.5 ml H_2O) in methanol (10 ml) was added concurrently in 30 min to a mixture of palladium(II) chloride (0.36 g), 2,2′-(ethylenediimino)dibenzaldehyde (0.27 g), and methanol (20 ml) under reflux with stirring. The reaction mixture was refluxed for another 1 h with stirring, and cooled down with ice–water. The crystalline solid was recovered and extracted with chloroform (30 ml); upon addition of a 10-fold amount of methanol red needles were obtained; yield 0.09 g (23%). Found: C, 54.39; H, 4.49; N, 13.76%; M+, 396.[7] Calcd for $C_{18}H_{18}N_4Pd$: C, 54.49; H, 4.57; N, 14.12%, M, 396.77.

Spectral Measurements. Ultraviolet and visible spectra were recorded on a Shimadzu UV-200S double beam spectrophotometer at room temperature. Infrared spectra covering the 650—4000 cm^{-1} range were measured with a JASCO IRA-2 grating spectrophotometer at room temperature. A JEOL JNM-FX 60 spectrometer was used to obtain NMR spectra at room temperature and chemical shifts were reported in ppm from internal TMS. ESR spectra were recorded at room temperature on a JEOL JES-ME-1 X-band and a JEOL JES-ME-3 K-band spectrometer equipped with a 100 kHz field modulation unit. The copper(II) and oxovanadium(IV) complexes of **1** were doped in ($\approx$1 wt%) the isomorphous ligand, while the metal complexes of **2** were in ($\approx$1 wt%) the isomorphous nickel complex for measurements. All the ESR sensitive metal complexes were also measured in xylene–benzene (2 : 1 v/v) at room temperature. The manganese ion diffused into magnesium oxide was used to obtain standard reference signals for measurements. ESCA spectroscopy was performed on a Du Pont 650B spectrometer using a Mg $K\alpha$ irradiation unit. A signal due to Au $4f_{5/2,7/2}$ was used for calibration.

Results and Discussion

Electronic Spectra. Visible and ultraviolet spectra covering the 16000—32000 cm^{-1} region are shown in Figs. 1 and 2 for the metal chelates of 5,14-dihydrodibenzo[*b,i*][1,4,8,11]tetraazacyclotetradecine (**1**) and 7,8,15,16,17,18-hexahydrodibenzo[*b,j*][1,4,8,11]tetraazacyclotetradecine (**2**), respectively, and the absorption bands appearing in the energy region greater than 16800 cm^{-1} are reasonably attributed to $\pi \rightarrow \pi^*$ transitions within a ligand molecule and charge-transfer transitions from metal to ligand. General feature of the spectra for the 16π-macrocycle (**1**) system is similar to those observed for metal porphyrins.[9,10] An extremely intense absorption band observed in the 23000—26000 cm^{-1} region is assigned to the so-called Soret-type transition, and a pair of weaker bands in the 19000—24000 cm^{-1} region are to the α- and β-type transitions (Table 1). The α, β, and Soret bands for the metal chelates of **1** are located in a higher energy region than those for the corresponding metal porphyrins. The oxovanadium(IV), nickel(II), copper(II), and palladium(II) complexes do not show any significant absorption in the region lying below *ca.* 17000 cm^{-1}. The spectral behavior is consistent with the square-planar coordination.[11]

The spectral features for the metal complexes of 12π-macrocycle **2** are quite different from those for metal porphyrins. The nickel(II) complex shows a spectrum similar to those observed for the nickel(II)–amben complex (**3**).[5,12,13] It is rather difficult at present to make exact assignments of absorption bands observed

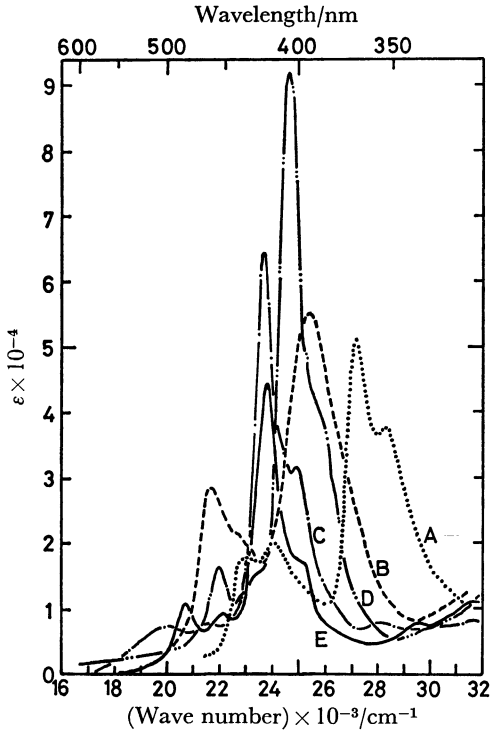

Fig. 1. Electronic absorption spectra of 5,14-dihydrodibenzo[*b*,*i*][1,4,8,11]tetraazacyclotetradecine chelates in *N*,*N*-dimethylformamide at room temperature.
A: Ligand, B: oxovanadium(IV), C: nickel(II), D: copper(II), E: palladium(II).

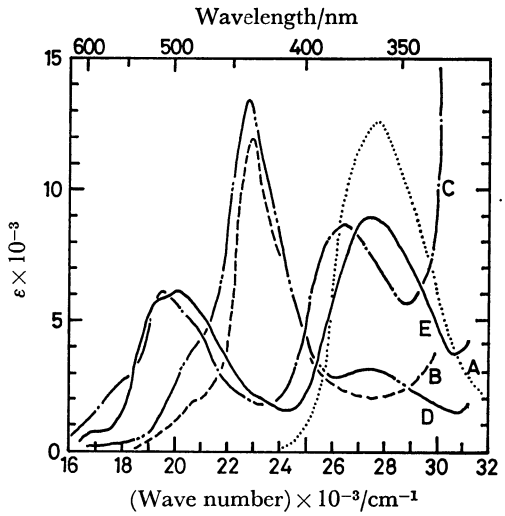

Fig. 2. Electronic absorption spectra of 7,8,15,16,17,18-hexahydrodibenzo[*b*,*j*][1, 4, 8, 11] tetraazacyclotetradecine chelates in benzene at room temperature.
A: Ligand, B: oxovanadium(II), C: nickel(II), D: copper(II), E: palladium(II).

in the visible and near UV regions, we tentatively assign intensive bands in the 18000—30000 cm^{-1} region

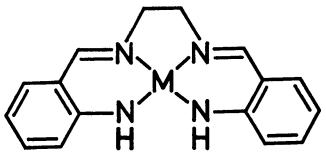

3

to charge-transfer and/or $\pi \rightarrow \pi^*$ transitions (Table 1). A low energy band, which is attributable to a ligand-field transition was observed only for the copper(II) and palladium(II) at 16900 (ε 700) and 15400 (ε 220) cm^{-1}, respectively.

Vibrational Spectra. The characteristic IR absorption bands for the present discussion are summarized in Table 2 together with those for Ni(amben)[13] and Ni(porphine).[14] The metal-free macrocycles show a weak band at *ca.* 3200 cm^{-1} which is associated with a N–H stretching mode in a manner as observed for the metal-free porphyrins.[15] This vibrational mode disappears upon complex formation.

A strong absorption band observed in the 1600 cm^{-1} region can be attributed to the stretching mode of C=N bond. This band is most sensitive to metal-coordination among the absorption peaks appearing in the NaCl region, and shifts significantly to lower frequency upon

Table 1. Characteristic absorption bands in the visible and near UV regions for the oxovanadium(IV), nickel(II), copper(II), and palladium(II) complexes of macrocycles **1** and **2**[a,b]

Metal	Transition energy in cm^{-1} (ε)			
	Macrocyclic ligand (**1**)[c]		Macrocyclic ligand (**2**)[d]	
	α-Band β-Band	Soret band	Charge-transfer/$\pi \rightarrow \pi^*$	
VO(IV)	21700 (28700) 22700sh (21600)	25400 (55600)	23000 (11900)	
Ni(II)	19900 (7200) 21600 (7620)	23600 (64400)	19600 (6110)	26500 (8680)
Cu(II)	22000 (16400) 23500sh (15740)	24700 (92100)	20800sh (4000) 27200 (3100)	22800 (13400)
Pd(II)	20700 (10900) 22100 (9570)	23800 (44600)	19600sh (5930) 20200 (6070)	27600 (8880)

a) **1**, 5,14-Dihydrodibenzo[*b*,*i*][1,4,8,11] tetraazacyclotetradecine; **2**,7,8,15,16,17,18-hexahydrodibenzo[*b*,*j*][1,4,8,11]tetraazacyclotetradecine. b) The most intense band observed for metal-free ligands: **1**, 27200 cm^{-1} (ε 51300); **2** 27800 cm^{-1} (ε 12700). c) Measured in *N*,*N*-dimethylformamide at room temperature. d) Measured in benzene at room temperature.

Table 2. Characteristic IR absorption bands for the oxovanadium(IV), nickel(II), copper(II), and palladium(II) complexes of macrocycles[a,b]

Ligand[c]	Metal	IR-band (cm^{-1})	Assignment	Ref.
1		1544(s)	$\nu_{C=C,C=N}$(macrocyclic skeletal)	
		1587(w)	$\nu_{C=C}$(conjugated ring)	
		1626(s)	$\nu_{C=N}$	
		3200(w)	ν_{N-H}	
1	VO^{IV}	967(s)	$\nu_{V=O}$	
		1448(s,br),1461(s,br)	$\nu_{C=C,C=N}$(macrocyclic skeletal)	
		1575(m)	$\nu_{C=N}$	
		1592(w)	$\nu_{C=C}$(conjugated ring)	
1	Ni^{II}	1460(s,br),1473(s,br)	$\nu_{C=C,C=N}$(macrocyclic skeletal)	
		1574(w)	$\nu_{C=N}$	
		1591(w)	$\nu_{C=C}$(conjugated ring)	
1	Cu^{II}	1452(m),1480(s,br)	$\nu_{C=C,C=N}$(macrocyclic skeletal)	
		1574(w)	$\nu_{C=N}$	
		1590(w)	$\nu_{C=C}$(conjugated ring)	
1	Pd^{II}	1440(s,br),1460(s,br)	$\nu_{C=C,C=N}$(macrocyclic skeletal)	
		1571(m)	$\nu_{C=N}$	
		1587(w)	$\nu_{C=C}$(conjugated ring)	
2		1581(s)	$\nu_{C=C,C=N}$(macrocyclic skeletal)	
		1623(s)	$\nu_{C=N}$	
		3260(w)	ν_{N-H}	
2	VO^{IV}	940(m)	$\nu_{V=O}$	
		1528(w)	$\nu_{C=C,C=N}$(macrocyclic skeletal)	
		1606(s)	$\nu_{C=N}$	
2	Ni^{II}	1509(w)	$\nu_{C=C,C=N}$(macrocyclic skeletal)	
		1606(s)	$\nu_{C=N}$	
2	Cu^{II}	1510(w)	$\nu_{C=C,C=N}$(macrocyclic skeletal)	
		1609(s)	$\nu_{C=N}$	
2	Pd^{II}	1510(w)	$\nu_{C=C,C=N}$(macrocyclic skeletal)	
		1601(s)	$\nu_{C=N}$	
Amben[d]	Ni^{II}	1537(s)	$\nu_{C=C}$(aromatic)	13
		1593(s)	$\nu_{C=N}$	
Porphine	Ni^{II}	1547(m)	$\nu_{C=C,C=N}$	14
		1547(m)	$\nu_{C=C}$	

a) Measured by KBr disk method at room temperature. b) Relative intensities: s, strong; m, medium; w, weak; br, broad. c) See Table 1 for numbering the ligands **1** and **2**. d) Amben, *N,N'*-ethylenebis(*o*-aminobenzylideneiminato).

metal-coordination. Such a spectral feature has been observed for Ni(amben),[13] but is not clear for metal porphyrins.[15] The magnitude of these frequency-shifts with respect to metal ions follows the sequence in an increasing order: Cu(II)≲VO(IV)≲Ni(II)≲Pd-(II). For the 5,14-dihydrodibenzo[*b,i*][1,4,8,11]tetra-azacyclotetradecine system, this characteristic band reduces its intensity to medium upon metal coordination. On the other hand, the C=N band observed for 12π-macrocyclic ligand **2** does not lose its intensity upon complex formation. The formation of a square-planar complex with higher conjugation system seems to be responsible for such reduction in IR activity.

A strong absorption band at around 950 cm^{-1} observed for the oxovanadium(IV) complexes is attributed to the V=O stretching mode.[16,17]

NMR Spectra. NMR data for macrocyclic ligands **1** and **2** and the nickel(II) and palladium(II) chelates of the latter ligand are listed in Table 3 along with the comparable data for Ni(II) ambtn,[13] zinc(II) dipyrromethene,[18] and nickel(II) porphyrin.[19,20] The complexes of macrocycle **1** are too insoluble to give satisfactory NMR spectra. The methine proton peak for **1** observed in the lower field region is shifted to down-field by *ca.* 1 ppm relative to that of dipyrromethenes (free base).[18] As the extent of down-field shift is smaller than that for porphyrins, the cyclic conjugation throughout the macrocyclic skeleton of **1** seems to be not so extensive as observed for porphyrins. In the case of **1**, the proton signals for methine groups (=CH–

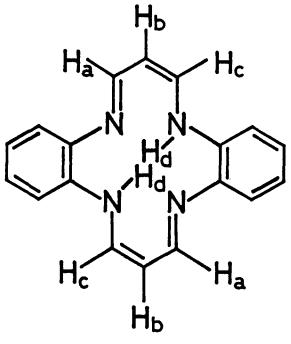

4

NH–, –CH=N–) of the 6-, 8-, 15-, and 17-positions were observed as a quintet. The H_a-methine proton (–CH=N–) shown by **4** couples with the H_b-methine proton (–CH=CH–), and the H_a-signal is split into a symmetrical doublet. On the other hand, the H_c-methine proton (–CH=NH–) couples both with H_b-(–CH=CH–) and H_d- (N–H), the H_c-signal being split into a triplet. Consequently, the quintet signal is referred to the overlap of a doublet and a triplet signal. The coupling of H_b- (–CH=CH–) with H_a- and H_c- seems to result in a triplet signal for H_b. A signal for the H_d-amine proton (N–H) was observed as a broad triplet with equal intensity due to coupling with the nitrogen nucleus ($I=1$).

The signal (9.27 ppm) for protons attached to the aniline-type nitrogen in **2** was found to disappear upon metal-coordination. The methine proton peak (8.32 ppm) observed for macrocycle **2** in the lowest field is shifted to up-field by 0.3 (palladium complex)—0.6 ppm (nickel complex) upon complex formation. This up-field shift is comparable to that observed for the meso-methine protons of nickel(II) porphyrin (Table 3).[19] This may be attributed to reduction of the ring current by incorporation of the nickel or the palladium. The shielding effect by nickel(II)-coordination is larger than that by palladium(II)-coordination. The metal-free macrocycle (**2**) showed the H_a-signal (refer to **5**) in the highest field (3.37 ppm) with some broadening. Upon substitution of the H_b proton on the nitrogen(–NH–) with deuterium(D), the H_a-signal at 3.37 ppm turned to be sharp. A similar spectral change was observed upon nickel(II)- and palladium(II)-coordination. Accordingly, the H_a protons(–CH_2–NH–) placed at the 16- and 17-positions must couple with the H_b protons(–CH_2–NH–) placed at the 15- and 18-positions, and the H_a protons absorption is observed as a broad signal owing to a small proton spin-coupling constant (J_{ab}). The H_a- and H_c-signals(=N–CH_2–, –CH_2–NH–) show down-field shift upon formation of the palladium chelate. These down-field shifts can be attributed to the deshielding effect provided by the positive charge on palladium-(II). The H_a- and H_c-(methylene protons) peaks are shifed to up-field upon formation of the nickel(II) complex. These up-field shifts can be attributed to the significant shielding effect provided by the chelate rings rather than the deshielding effect due to the positive charge on nickel(II). This seems to indicate that the methylene groups of the nickel(II) complex are placed in a conformational space different from that occupied by those of the palladium(II) complex, most likely due to the difference in ionic radius between Ni^{2+} and Pd^{2+}.

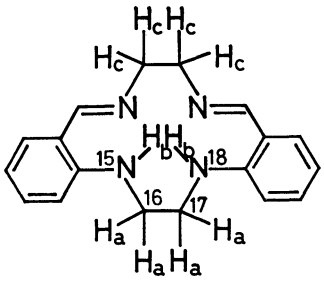

5

ESCA Spectra. For macrocyclic ligands **1** and **2** and their complexes, binding energies of carbon(C $1s_{1/2}$), nitrogen(N $1s_{1/2}$), vanadium(V $2p_{1/2}$, $2p_{3/2}$), oxygen(O $1s_{1/2}$), nickel(Ni $2p_{1/2}$, $2p_{3/2}$), copper(Cu $2p_{1/2}$, $2p_{3/2}$), and palladium(Pd $3p_{1/2}$, $3p_{3/2}$) are listed in Tables 4 and 5 together with those for 5,10,15,20-tetraphenylporphine, phthalocyanine, and their copper(II) complexes.[21] There are these possible structure as to the location of inner hydrogen atoms in macrocycles **1** and **2** (Fig. 3). Macrocyclic ligand **1** shows two N 1s peaks

TABLE 3. PROTON NMR DATA FOR NICKEL(II), AND PALLADIUM(II) COMPLEXES OF MACROCYCLES[a]

Ligand[b]	Sample	Amine –NH	Methine =CH–NH–	Methine –CH=N–	Methine –CH=C–	Aromatic	Methylene =N–CH_2–	Methylene –CH_2–NH–	Methylene –CH_2–C–	Ref.
1	ligand[e]	13.63(3)[e] (J=6.2Hz)	7.664(3)[e] (J=6.2Hz)	7.657(2)[e] (J=6.2Hz)	4.97(3)[e] (J=6.2Hz)	7.13—6.73(m)				
2	ligand[d]	9.27br		8.32		7.47—6.43(m)	3.76	3.37br		
2	Ni-chelate[d]			7.74		7.37—6.13(m)	3.49	3.36		
2	Pd-chelate[d]			7.99		7.53—6.20(m)	3.85	3.75		
MP	ligand[d]	−3.91			10.095					19,20
MP	Ni-chelate[d]				9.805					19
Ambtn	Ni-chelate[d]	6.06br		7.64		7.2—6.4(m)	3.53(3)[e] (J=6.0Hz)		1.85(5)[e] (J=6.0Hz)	13
DM	ligand				6.62					18
DM	Zn-chelate[d]				6.98					18

a) Chemical shifts are given in ppm for TMS. b) MP, mesoporphyrin IX dimethyl ester; Ambtn, *N,N'*-trimethylene-bis(*o*-aminobenzylideneiminato); DP, 3,3',4,4',5,5'-hexamethyldipyrromethene. c) Measured in dimethyl sulfoxide-d_6 with TMS as an internal reference. d) Measured in chloroform-*d* with TMS as an internal reference. e) Multiplicity of a proton signal is given in parentheses after δ-value.

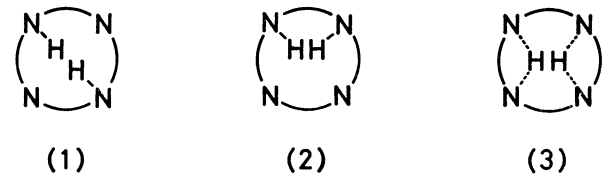

(1) (2) (3)

Fig. 3. Three possible structures arising from the location of inner hydrogen atoms of macrocycles.
(1) Two inner hydrogen atoms are directly bound to diagonally opposite nitrogen atoms.
(2) Two inner hydrogen atoms are fixed to adjacent nitrogen atoms.
(3) Two inner hydrogen atoms are shared by four equivalent central nitrogen atoms.

(396.0, 397.2 eV) (Table 4) with nearly equal intensity. The general feature of a nitrogen 1s peak is similar to those observed for porphyrins and phthalocyanine.[21,23-25] Moreover, the ^{1}H-NMR spectrum shows the presence of two kinds of nitrogen atoms as judged by the methine proton signal (Table 3). Consequently, there are two kinds of nitrogen atoms in macrocycle **1**; the one without hydrogen atom, and the other with hydrogen attached. Our result rules out any structure with hydrogen bridges, yielding equivalent nitrogens (Fig. 3-(3)), although the possibility of forming intramolecular hydrogen bonding is not eliminated. A structure of type(2) in Fig. 3 must be ruled out, since this destroys π-conjugation of the ligand. The most plausible molecular structure for macrocycle **1** is type(1) in Fig. 3; two inner hydrogen atoms are bound to nitrogen at diagonal positions.

Since macrocyclic ligand **2** shows only one N 1s peak at 397.5 eV as shown in Table 4, this feature is different from those observed for porphyrins, phthalocyanine, and macrocycle **1**. The tautomeric effect (refer to **6**) which provide only equivalent nitrogens seems to be responsible for the existance of one N 1s signal (type(3) in Fig. 3).

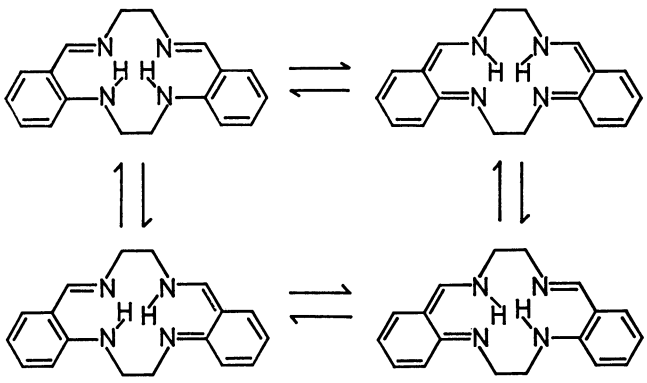

6

As shown in Table 4, only one N 1s peak was observed for the macrocyclic chelates; namely, the four nitrogens are chemically equivalent in these complexes. The nitrogen 1s peak observed in the 397—398 eV region for the bivalent metal chelates does not appreciably vary the peak position by changing metal species as

Table 4. Carbon and nitrogen core-electron binding energies for macrocyclic and their metal complexes[a]

Ligand[b]	Sample	Binding energy in eV		Ref.
		C $1s_{1/2}$	N $1s_{1/2}$	
1	ligand	282.7	396.0,397.2	
1	VO-chelate	283.5	397.3	
1	Ni-chelate	284.0	397.8	
1	Cu-chelate	284.0	397.7	
1	Pd-chelate	283.9	397.9	
2	ligand	283.8	397.5	
2	VO-chelate	284.0	397.8	
2	Ni-chelate	283.9	397.4	
2	Cu-chelate	283.4	396.8	
2	Pd-chelate	283.8	397.6	
TPP	ligand	284.8	398.2,400.2	21
TPP	Cu-chelate	284.8	398.9	21
PC	ligand	284.8,286.2	398.9,400.4	21
PC	Cu-chelate	284.8,286.2	399.2	21

a) Measured in the tablet state (5-mm diameter); for calibration, the signal of Au $4f_{5/2}$ and Au $4f_{7/2}$ was used.
b) See Table 1 for numbering the ligands **1** and **2**; TPP, 5,10,15,20-tetraphenylporphine; PC, phthalocyanine.

shown in Table 4. Our result is comparable to those obtained for porphyrins.[21,23-25] The N 1s peak for porphyrins and phthalocyanine is somewhat shifted to higher energy because of high π-conjugation.

ESR Spectra. Oxovanadium(IV) Complex: In the ESR spectra of macrocyclic oxovanadium(IV) complexes measured in xylene–benzene (2 : 1 v/v) at room temperature, a set of eight hyperfine lines were observed by the magnetic interaction between an unpaired electron and vanadium nucleus (I=**7/2**). The similar spectral features have been observed for (5,10,15,20-tetraphenylporphinato) oxovanadium (IV) complex.[26] Figure 4 shows the ESR spectrum recorded at room temperature for the powdered sample of (dibenzo[*b*,*i*]-[1,4,8,11]tetraazacyclotetradecinato)oxovanadium(IV) magnetically diluted with the corresponding ligand as an example. This spectrum is composed of two sets of vanadium hyperfine lines; $g_{//}$ and $g_{\perp}$ components.

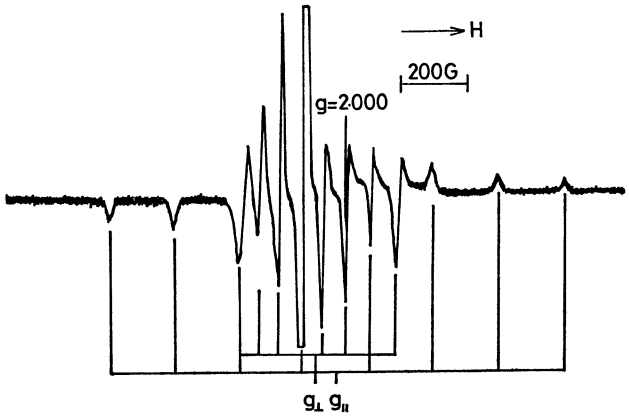

Fig. 4. ESR spectrum of (dibenzo[*b*, *i*][1, 4, 8, 11]tetraazacyclotetradecinato)oxovanadium(IV) complex magnetically diluted with the corresponding metal-free ligand at room temperature.

TABLE 5. METAL 2p, 3p, AND OXYGEN 1s BINDING ENERGIES FOR METAL-MACROCYCLIC COMPLEXES[a)]

Compound[b)]	Binding energy in eV								
	V $2p_{1/2}$	V $2p_{3/2}$	O $1s_{1/2}$	Ni $2p_{1/2}$	Ni $2p_{3/2}$	Cu $2p_{1/2}$	Cu $2p_{3/2}$	Pd $3p_{1/2}$	Pd $3p_{3/2}$
V-metal	520[c)]	513[c)]							
O			532[c)]						
1-VO-chelate	521.8	514.8	529.3						
2-VO-chelate	522.1	514.6	531.2						
Ni-metal				872[c)]	855[c)]				
1-Ni-chelate				871.0	853.5				
2-Ni-chelate				871.1	853.9				
Cu-metal						951[c)]	931[c)]		
1-Cu-chelate						953.0	933.1		
2-Cu-chelate						953.0	933.0		
Pd-metal								559[c)]	531[c)]
1-Pd-chelate								557.0	531.5
2-Pd-chelate								561.7	534.1

a) Measured in the tablet state (5-mm diameter); for calibration, the signal of Au $4f_{5/2}$ and Au $4f_{7/2}$ was used. b) See Table 1 for numbering the ligands. c) Values reported in Ref. 22.

The superhyperfine splitting, due to magnetic interaction between an unpaired electron in V(IV) and nitrogen nuclei(I=**1**), has not been observed in the present oxovanadium(IV) complexes. Consequently, the oxovanadium(IV) complexes are of square-planar type with an unpaired electron in the $d_{x'-y'}$ orbital. The similar spectral features have also been observed for the complexes derived from porphyrins[26-28] and phthalocyanine.[29] A plausible structure around the coordination site for the oxovanadium(IV) complexes are illustrated schematically by (**7**) except for V=O on

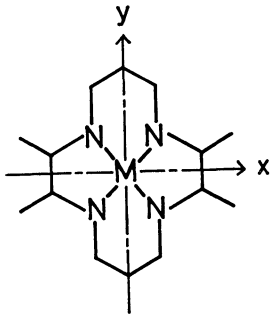

7

z-axis. Since the spin-orbit coupling constant is much smaller than the orbital excitation energies, the first-order perturbation can be applied to our system for evaluation of g values

$$g_z = g_0 - 8\lambda/\Delta_3 = g_{\parallel} \quad (1)$$

$$\left.\begin{aligned} g_x &= g_0 - 2\lambda/\Delta_2 \\ g_y &= g_0 - 2\lambda/\Delta_1 \end{aligned}\right\} = g_{\perp} \quad (2), (3)$$

where $\Delta_3=\Delta E(d_{xy}\leftarrow d_{x'-y'})$, $\Delta_2=\Delta E(d_{xz}\leftarrow d_{x'-y'})$, $\Delta_1=\Delta E(d_{yz}\leftarrow d_{x'-y'})$, and λ is the spin-orbit coupling constant of V^{4+} ion. The g ($g_{//}$ and $g_{\perp}$) and A ($A_{//}$ and $A_{\perp}$) values for the oxovanadium(IV) complex of macrocycle **1** are in agreement with those obtained for the complex of macrocycle **2** as shown in Table 6. The $g_{//}$ and $g_{\perp}$ values in this work are slightly larger in magnitude than those obtained for the complexes of 5,10,15,20-tetraphenylporphine and phthalocyanine, but the $A_{//}$ and $A_{\perp}$ values are smaller.[26,29] The $|g_0-g_{//}|$ values in this work are comparable to those obtained for the complexes of 5,10,15,20-tetraphenylporphine[26] and phthalocyanine.[29] This may be attributed to equivalent Δ_3 (refer to Eq. 1) value for the complexes of the present macrocycles, 5,10,15,20-tetraphenylporphine, and phthalocyanine. The $|g_0-g_{\perp}|$ values in this work are smaller in magnitude than those obtained for the complexes of 5,10,15,20-tetraphenylporphine and phthalocyanine (Table 6). On the basis of Eqs. 2 and 3, the Δ_1 and Δ_2 values obtained in this work are larger than those for the complexes of 5,10,15,20-tetraphenylporphine and phthalocyanine. Namely, the relative energy level of d_{xy}, d_{yz} is higher than those estimated for the 5,10,15,20-tetraphenylporphine and phthalocyanine complexes.

Copper(II) Complex. The ESR spectra of (dibenzo[*b*,*i*][1,4,8,11]tetraazacyclotetradecinato) copper(II) magnetically diluted with the corresponding metal-free ligand at room temperature are shown in Fig. 5 as an example. The general feature of spectra (A) and (B) is similar to that observed for the square-planar copper(II) complexes derived from porphyrins[26,30] and phthalocyanine.[31] In these two spectra, a set of four copper hyperfine lines on the parallel component of the g-tensor($g_{//}$), which lie in the low field region, are observed, while such hyperfine lines are not obvious on the perpendicular component of the g-tensor($g_{\perp}$) in the higher field region. The X- and K-band ESR spectra shown in Fig. 5 indicates that the $g_{\perp}$-tensor is of anisotropic nature; D_{2h} coordination symmetry. In addition, superhyperfine lines due to four chemically equivalent nitrogen donor atoms, appear on the perpendicular component of the g-tensor($g_{\perp}$, g_2, and g_3) at higher field, while such superhyperfine lines are not observed on the parallel component of the g-tensor($g_{//}$) at lower field. As judged from the general feature of superhyperfine lines, it may be concluded that an unpaired electron of the copper(II)

TABLE 6. SPIN HAMILTONIAN PARAMETERS FOR OXOVANADIUM(IV) AND COPPER(II) COMPLEXES OF MACROCYCLES[a,b]

Ligand[c]	Metal	Medium	$\bar{g}$	$\lvert g_0-g_{//}\rvert$	$\lvert g_0-g_{\perp}\rvert$	$\bar{A}\times 10^4\mathrm{cm}^{-1}$	$A_{//}\times 10^4\mathrm{cm}^{-1}$	$A_{\perp}\times 10^4\mathrm{cm}^{-1}$	$A_{\perp}^{N}\times 10^4\mathrm{cm}^{-1}$	Ref.
1[f]	VO	xylene–benzene[d]	1.989			86.1				
1[f]	VO	ligand(**1**)[e]		0.035	0.004		150.0	52.8		
2[f]	VO	xylene–benzene[d]	1.989			86.3				
2[f]	VO	Ni(II)complex[e]		0.031	0.003		149.4	53.2		
H_2TPP[f]	VO	$CHCl_3$	1.9797			89.4				26
H_2TPP[f]	VO	H_2TPP[e]		0.036	0.017		161	55		26
1[f]	Cu	xylene–benzene[d]	2.089			96.4				
1[f]	Cu	ligand(**1**)		0.128	0.033,0.010		218.0		7.3	
1[g]	Cu	ligand(**1**)		0.126	0.029,0.009		219.0		7.1	
2[f]	Cu	xylene–benzene[d]	2.089			96.0				
2[f]	Cu	Ni(II)complex[e]		0.133	0.040,0.008		208.7		15.6	
H_2TPP[f]	Cu	$CHCl_3$	2.1073			97.7			15.9	26
H_2TPP[f]	Cu	H_2TPP[e]		0.191	0.069		202		14.5	26

a) Measured at room temperature. b) Maximum possible essors: g, ± 0.0005; $\bar{A}, A_{//}$, $\pm 0.5\times 10^{-4}$ cm^{-1}; $A_{\perp}, A_{\perp}^{N}$, $\pm 0.05\times 10^{-4}$cm^{-1}. c) See Table 1 for numbering the ligands **1** and **2**; H_2TPP, 5,10,15,20-tetraphenylporphine. d) Concentration of the complex, 10^{-3}—10^{-4} mol/l (xylene–benzene; 2: 1 v/v). e) (7,8,16,17-Tetrahydrodibenzo[*b*, *j*] [1,4,8,11] tetraazacyclotetradecinato)nickel(II)complex. f) X-Band microwave. g) K-Band microwave.

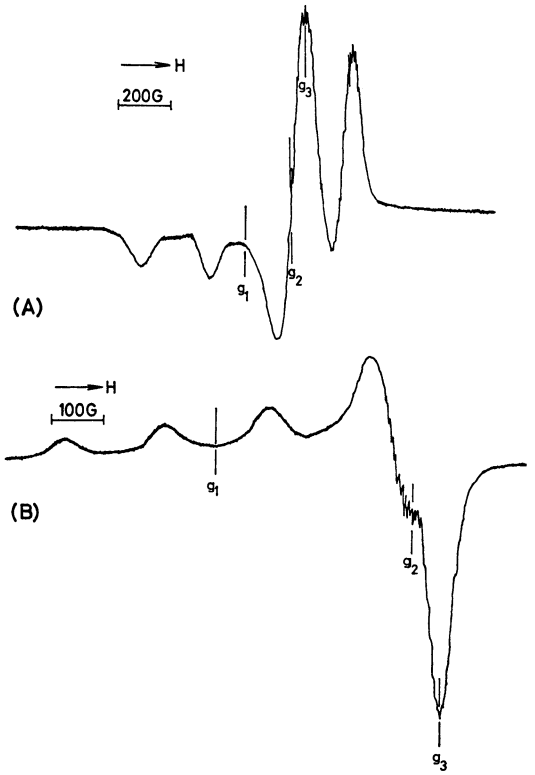

Fig. 5. ESR spectrum of (dibenzo[*b*,*i*][1,4,8,11]tetraazacyclotetradecinato)copper (II) complex magnetically diluted with the corresponding metal-free ligand at room temperature.
(A): X-Band microwave, (B): K-band microwave.

complex is placed in its d_{xy} orbital.

Although the $g_{//}$ and $g_{\perp}$ values are somewhat smaller in magnitude than those observed for the complexes derived from porphyrins[26,30] and phthalocyanine,[31] the Δg value ($\Delta g=g_{//}-g_{\perp}$) is approximately equal in magnitude to those of porphyrin complexes and phthalocyanine complex. Moreover, the $A_{//}$ value is somewhat larger in magnitude than those reported for porphyrin complexes[26,30] and phthalocyanine complex.[31] This is attributed to the greater electron density of the unpaired electron of copper(II) nucleus. The K-band ESR spectrum for the magnetically diluted powdered sample indicates the presence of three g values such as g_z, g_y, g_x as shown in Fig. 5-(B). If the coordination symmetry is D_{2h} (refer to **7**), these values are expected to be $g_z > g_y$, g_x ($g_x \neq g_y$). On this basis, the copper atom most plausibly assumes a distorted square-planar coordination of Cu–N_4 type due to the presence of five- and six-membered chelate rings. Furthermore, the five- and six-membered chelate rings are placed in the same plane, so that efficient π-conjugation is attained in the macrocyclic ligand moiety. The $A_{\perp}^{N}$ value for the complex of macrocycle **1** is about a half of the one observed for the complexes derived from porphyrins[26,31] and phthalocyanine,[31] but the $A_{\perp}^{N}$ value for the complex of macrocycle **2** is similar in magnitude to those for the porphyrins and phthalocyanine complexes. Consequently, the metal d-electrons in the copper(II) complex are more delocalized toward the ligand moiety through the coordinate bonds in a manner as expected for the corresponding complexes of **2**.

References

1) J. E. Falk, "Porphyrins and Metalloporphyrins," Elsevier Publishing Co., Amsterdam (1964).
2) For dehydrocorrins and corroles: (a) Y. Murakami, K. Sakata, Y. Tanaka, and T. Matsuo, *Bull. Chem. Soc. Jpn.*, **48**, 3622 (1975); (b) Y. Murakami and Y. Aoyama, *Bull. Chem. Soc. Jpn.*, **49**, 683 (1976); (c) Y. Murakami, S. Yamada, Y. Matsuda, and K. Sakata, *Bull. Chem. Soc. Jpn.*, **51**, 123 (1978); (d) N. S. Hush and I. S. Woolsey, *J. Am. Chem. Soc.*, **94**, 4107 (1972); (e) N. S. Hush and I. S. Woolsey, *J. Chem. Soc., Dalton Trans.*, **1972**, 24. For corrins: (f) J. M. Pratt, "Inorganic Chemistry of Vitamin B_{12}," Academic Press, London (1972).
3) T. J. Truex and R. H. Holm, *J. Am. Chem. Soc.*, **94**, 4529 (1972).
4) H. Hiller, P. Dimroth, and H. Pfitzner, *Liebigs Ann. Chem.*, **717**, 137 (1968).

5) M. Green and P. A. Tasker, *Inorg. Chim. Acta*, **5**, 65 (1971).
6) C. Sauer, *Org. Synth.*, Coll. Vol. IV, 813 (1963).
7) Mass spectral measurements were carried out with a GCMS-9000 gas chromatograph-mass spectrometer.
8) M. Green, J. Smith, and P. A. Tasker, *Inorg. Chim. Acta*, **5**, 17 (1971).
9) L. Edwards, D. H. Dolphin, and M. Gouterman, *J. Mol. Spectrosc.*, **35**, 90 (1970).
10) C. Weiss, H. Kobayashi, and M. Gouterman, *J. Mol. Spectrosc.*, **16**, 415 (1965).
11) A. B. P. Lever, "Inorganic Electronic Spectroscopy," Elsevier Publishing Co., Amsterdam (1968).
12) M. Green and P. A. Tasker, *Discuss. Faraday. Soc.*, **47**, 172 (1969).
13) M. Green and P. A. Tasker, *J. Chem. Soc., A*, **1970**, 2531.
14) H. Ogoshi, Y. Saito, and K. Nakamoto, *J. Chem. Phys.*, **57**, 4194 (1972).
15) L. J. Boucher and J. J. Katz, *J. Am. Chem. Soc.*, **89**, 1340 (1967).
16) K. Nakamoto, "Infrared Spectra of Inorganic and Coordination Compounds," John Wiley and Sons, Inc., New York (1970), p. 114.
17) J. G. Erdman, V. G. Ramsey, N. W. Kalenda, and W. E. Hanson, *J. Am. Chem. Soc.*, **78**, 5844 (1956).
18) Y. Murakami and K. Sakata, *Bull. Chem. Soc. Jpn.*, **47**, 3025 (1974).
19) D. A. Doughty and C. W. Dwiggins, Jr., *J. Phys. Chem.*, **73**, 423 (1969).
20) E. D. Becker, R. B. Bradley, and C. J. Watson, *J. Am. Chem. Soc.*, **83**, 3743 (1961).
21) Y. Niwa, H. Kobayashi, and T. Tsuchiya, *J. Chem. Phys.*, **60**, 799 (1974).
22) K. Siegbahn, C. Nordling, A. Fahlman, R. Nordberg, K. Hamrin, J. Hedman, G. Johansson, T. Bergmark, S. E. Karlsson, I. Lindgran, and B. Lindberg, "Electrion Spectroscopy for Chemical Analysis-Atomic, Molecular, and Solid State Structure Studies by Means of Electron Spectroscopy," Almqvist and Wiksell, Uppsala (1969).
23) M. V. Zeller and R. G. Hayes, *J. Am. Chem. Soc.*, **95**, 3855 (1973).
24) D. Karweik, N. Winograd, D. G. Davis, and K. M Kadish, *J. Am. Chem. Soc.*, **96**, 591 (1974).
25) J. P. Macquet, M. M. Millard, and T. Theophanides, *J. Am. Chem. Soc.*, **100**, 4741 (1978).
26) J. M. Assour, *J. Chem. Phys.*, **43**, 2477 (1965).
27) E. M. Roberts, W. S. Koski, and W. S. Caughey, *J. Chem. Phys.*, **34**, 591 (1961).
28) D. Kivelson and S. K. Lee, *J. Chem. Phys.*, **41**, 1896 (1964).
29) J. M. Assour, J. Goldmacher, and S. E. Harrison, *J. Chem. Phys.*, **43**, 159 (1965).
30) E. M. Roberts and W. S. Koski, *J. Am. Chem. Soc.*, **82**, 3006 (1960).
31) D. Kivelson and R. Neiman, *J. Chem Phys.*, **35**, 149 (1961).